

OMAE2015-42361

SENSITIVITY OF ROGUE WAVE PREDICTION TO OCEANIC STRATIFICATION

Qiuchen Guo

Department of Mechanical Engineering
University of California Berkeley
Berkeley, California 94720
Email: qiuchen@berkeley.edu

M.-Reza Alam

Department of Mechanical Engineering
University of California Berkeley
Berkeley, California 94720
Email: reza.alam@berkeley.edu

ABSTRACT

Oceanic rogue waves are short-lived very large amplitude waves (a giant crest typically followed or preceded by a deep trough) that appear and disappear suddenly in the ocean causing damage to ships and offshore structures. Assuming that the state of the ocean at the present time is perfectly known, then the upcoming rogue waves can be predicted via numerically solving the equations that govern the evolution of the waves. The state of the art radar technology can now provide accurate wave height measurements over large spatial domains and when combined with advanced wave-field reconstruction techniques together render deterministic details of the current state of the ocean (i.e. surface elevation and velocity field) at any given moment of time with a very high accuracy. The ocean density is, however, stratified (mainly due to the salinity and temperature differences). This density stratification, with today's technology, is very difficult to measure accurately. As a result in most predictive schemes these density variations are neglected. While the overall effect of the stratification on the average state of the ocean may not be significant, here we show that these density variations can strongly affect the prediction of oceanic rogue wave. Specifically, we consider a broadband oceanic spectrum in a two-layer density stratified fluid, and study via extensive statistical analysis the effects of strength of the stratification (difference between densities) and the depth of the thermocline on the prediction of upcoming rogue wave.

INTRODUCTION

Oceanic rogue waves, also known as freak waves, extreme waves or monster waves, are extreme events occurring in the ocean featured by a giant crest followed or preceded by a deep trough. The term *rogue wave* was first introduced by Draper [1] [2]. Mathematically speaking, a rogue wave is a wave whose height exceeds twice the significant wave height of the spectrum. Although rogue waves are extreme statistical events, accidents caused by rogue waves are reported every year [3–5]. Rogue waves act like a wall of water or a deep localized depression in the surface. Rogue waves can be extremely dangerous because they usually exceed the design load consideration of offshore structures and ships [6]. The exact mechanism behind the formation of rogue waves is still a matter of dispute [7].

Rogue waves can occur both in shallow water and deep water. Various mechanisms have been proposed to explain the formation of rogue waves under different circumstances. The abnormal local wave focusing can be caused by strong wind blowing over the sea surface [8], such as storm. Wave energy can also get focused by interacting with currents [9]. Nonlinearity may produce instability of wave field and lead to extreme waves in a relatively calm background wave field [3].

The density of water in an ocean or a sea is typically not constant. The variation of density is due to, mainly, variations of temperature and salinity. Solar radiation heats up the upper layer of the water, and the flow of rivers and the melting of ice lower the water density near the surface. Over time these effects add up to form a stable density stratification with the lighter fluid on top and the denser fluid below it. Stratified waters, besides

regular surface waves, admit the so-called *internal wave* which are gravity waves that propagate within the body of the water [10].

Field observations have reported ubiquitously non-uniform vertical gradients of stratification in the oceans: water density is nearly constant in an upper layer (epilimnion) and then jumps, over a (relatively) thin layer of sudden density change- the so called thermocline-, to a denser lower layer fluid (hypolimnion). Density stays almost constant below the thermocline to the ocean floor [11]. Therefore for ocean scenarios a two-layer model, with the density of each layer constant within the layer, is plausible and widely used. If a two-layer density stratification assumption is employed, internal waves are restricted to propagate on the thermocline only. These waves, sometimes also called interfacial waves, are widely observed in the oceans, seas and lakes [10, 12–14].

The purpose of this research is to investigate how oceanic rogue waves predictions are affected by the density stratification. Specifically, we consider scenarios in which a rogue waves is anticipated in a homogeneous fluid, and investigate, statistically, how much error is imposed if the density is variable. We specifically consider a two-layer density stratified setup. We study the error as a function of strength of stratification (i.e. the ratio of density of upper layer to that of the lower layer) and the depth of the thermocline.

PROBLEM FORMULATION

In order to compare the predicted rogue waves in both homogeneous fluid and stratified fluid, the governing equations and boundary conditions are formulated in both models. In homogeneous fluid (density ρ is constant), the problem is formulated in a Cartesian coordinate with x, y axis as the horizontal axis located on the mean surface and the z axis as vertical axis with positive upward. Under the assumption of incompressible fluid, irrotational and inviscid flow, velocity u can be expressed in terms of velocity potential with $u = \nabla\phi$. Surface tension is ignored. The governing equations and boundary conditions are:

$$\nabla^2\phi = 0, \quad -h < z < \eta(x, t) \quad (1a)$$

$$\phi_{tt} + g\phi_z + [\partial_t + 1/2(\nabla\phi \cdot \nabla)](\nabla\phi \cdot \nabla\phi) = 0, \quad z = \eta(x, t) \quad (1b)$$

$$g\eta + \phi_t + 1/2(\nabla\phi \cdot \nabla\phi) = 0, \quad z = \eta(x, t) \quad (1c)$$

$$\phi_z = 0, \quad z = -h \quad (1d)$$

where $\eta(x, t)$ is the surface elevation, h is constant depth of the ocean and g is the gravity acceleration. For a given initial condition, the wave field characteristics, including wave elevation and velocity potential, are obtained by solving the wave evolution equation.

Phase resolved high-order spectral(HOS) method is used in solving the governing equations. HOS is originally developed by Dommermuth & Yue [15, 16] for nonlinear wave-wave and wave-bottom interactions in the homogeneous fluid. The velocity potential can be expressed in perturbation series. Thus the governing equations can be solved by collecting terms with the same order together with initial conditions.

Now we consider a two-layer density stratified fluid model. Let's assume that the subscript u denotes the physical quantities in upper layer and the subscript ℓ denotes those in lower layer. For example, the upper layer and lower layer have respectively mean depth h_u and h_ℓ and fluid density ρ_u and ρ_ℓ . The ocean has constant depth $h = h_u + h_\ell$. We assume that both upper layer and lower layer are homogeneous, incompressible, inviscid and irrotational. The surface tension is ignored. Thus the fluid velocity in each layer can be described by velocity potentials, ϕ_u and ϕ_ℓ . The governing equations, surface boundary conditions, interface boundary conditions and the bottom boundary condition are:

$$\nabla^2\phi_u = 0, \quad -h_u + \eta_\ell < z < \eta_u \quad (2a)$$

$$\nabla^2\phi_\ell = 0, \quad -h_u + h_\ell < z < -h_u + \eta_\ell \quad (2b)$$

$$\phi_{u,tt} + g\phi_{u,z} + [\partial_t + 1/2(\nabla\phi_u \cdot \nabla)](\nabla\phi_u \cdot \nabla\phi_u) = 0, \quad z = \eta_u \quad (2c)$$

$$g\eta_u + \phi_{u,t} + 1/2(\nabla\phi_u \cdot \nabla\phi_u) = 0, \quad z = \eta_u \quad (2d)$$

$$\begin{aligned} \mathcal{R}\{\phi_{u,tt} + g\phi_{u,z} + 1/2(\nabla\phi_u \cdot \nabla\phi_u)_t + \\ \eta_{\ell,t}[\phi_{u,t} + 1/2(\nabla\phi_u \cdot \nabla\phi_u)]_z \\ - g\eta_{\ell,x}\phi_{u,x}\} - \{\phi_{\ell,tt} + g\phi_{\ell,t} \\ + 1/2(\nabla\phi_\ell \cdot \nabla\phi_\ell)_t + \eta_{\ell,t}[\phi_{\ell,t} \\ + 1/2(\nabla\phi_\ell \cdot \nabla\phi_\ell)]_z - g\eta_{\ell,x}\phi_{\ell,x}\}, \quad z = -h_u + \eta_\ell \quad (2e) \end{aligned}$$

$$\eta_{\ell,t} + \eta_{\ell,x}\phi_{u,x} - \phi_{u,z} = 0, \quad z = -h_u + \eta_\ell \quad (2f)$$

$$\eta_{\ell,t} + \eta_{\ell,x}\phi_{\ell,x} - \phi_{\ell,z} = 0, \quad z = -h_u + \eta_\ell \quad (2g)$$

$$\phi_{\ell,z} = 0, \quad z = -h_u - h_\ell \quad (2h)$$

where η_u and η_ℓ are the surface and interface elevation respectively, $\mathcal{R} = \rho_u/\rho_\ell$ is the density ratio. (2a)-(2b) are the governing equations in the upper domain and lower domain respectively. (2c)-(2d) are the free surface boundary conditions. (2e)-(2g) are the interface boundary conditions. (2h) is the bottom boundary condition.

We consider a broadband spectrum of waves propagating in the ocean. The initial sea state is specified by the spectral density function $S(\omega)$, given by the JONSWAP (Joint North Sea Wave Project) spectrum originally developed by Hasselmann [17] according to wave data measured in the North Sea, west of Denmark, for wind driven seas. The JONSWAP spectrum is fitted to the measured spectra to provide values of the model parameters. The JONSWAP spectrum was primarily used to investigate the energy transfer in the spectral transformation, which has an

application in wave prediction. The spectral density function for the JONSWAP spectrum is given as

$$S(\omega) = \frac{\alpha_p g^2}{\omega^5} e^{\beta} \gamma^\delta \quad (3)$$

where $\alpha_p = H_s^2 \omega_p^4 / (16 I_0(\gamma) g^2)$, $\beta = -1.25(\omega_p / \omega)^4$ and $\delta = \exp[-(\omega - \omega_p)^2 / (2\omega_p \sigma^2)]$. H_s is the significant wave height, which is four times the standard deviation of the surface elevation. γ is the peak enhancement factor, ranging from 1 to 9. We choose $\gamma = 3.3$, which is the value typically chosen [18]. $I_0(\gamma)$ is the zeroth order moment and is obtained numerically. For the chosen γ , we have $I_0(3.3) = 0.3$. ω_p is the peak radial frequency of the spectrum and ω is the wave radian frequency. $\sigma = 0.07, 0.09$ for respectively $\omega \leq \omega_p$ and $\omega > \omega_p$.

The prediction of the wave field is realized by solving the evolution equations using the phase resolved high-order spectral method. This method is a pseudo-spectral method based on the Fast Fourier Transform algorithm. This method uses the Zakharov equation and boundary conditions to calculate velocities up to an arbitrary order of nonlinearity M in terms of wave steepness. It can also take into account a large number of wave modes $N = O(10^2 \sim 10^3)$. We expand ϕ_u and ϕ_ℓ in perturbation series up to order M . Then we can expand the surface and interfacial boundary conditions into a sequence of linearized boundary value problems for perturbed potentials. The detailed two layer problem formulation and HOS numerical scheme can be found in Alam's paper [19, 20]. The result converges exponentially with M and N up to wave steepness $kA \simeq 0.35$. The scheme has already undergone extensive convergence tests as well as validations against experimental and other numerical results [19–25].

PROBLEM IMPLEMENTATION AND RESULTS

The probability of rogue wave occurrence depends on the initial sea state, which determines the statistical characteristics of the free surface (wave height, period and spectrum). The World Meteorological Organization classifies the sea state into 10 levels, from sea state 0 to 9. Sea states 4, 5 and 6 represent moderate, rough and very rough sea states respectively. In this paper, sea state 5 (with $H_s = 3.25$ m and $T_p = 9.7$ s) is used to formulate the initial conditions, where T_p is the period of waves at the peak of the spectrum. We define the maximum crest to trough height of rogue waves as H_r , then we use the normalized variable $H_{rs} = H_r / H_s$ as a parameter measuring predicted rogue waves. Alam [26] showed that the limit of maximum H_{rs} ratio in sea state 4 is about 2.6. The ratio can reach values larger than 2.6 in sea state 5 and 6. For all the calculations here, H_s and T_p of sea state 5 are used to obtain the spectral density function $S(\omega)$. Then we use $S(k) = S(\omega)C_g(\omega)$ to change the spectral density from a function of frequency to wave number k , where

$C_g = d\omega/dk$ is the group velocity. Then we initialize the surface wave (specifying initial η and ϕ) by using a linear combination of N waves with random phases with uniform average ranging in the domain $[0, 2\pi)$. Spurious high-frequency wave modes arise when we use the linear solution as initial conditions to the nonlinear evolution equations. To resolve this problem, we multiply the nonlinear terms in the boundary conditions by a weight function $\hat{W}(t)$ to gradually introduce nonlinear boundary conditions within a predetermined time [27], chosen to be $t_{pre} = 5T_p$. $\hat{W}(t)$ varies from 0 to 1 gradually for $t \in [0, t_{pre}]$ and $\hat{W} = 1$ for $t > t_{pre}$.

If we successfully find a rogue wave at time $t = t_i$ with peak at location $x = x_i$, we then continue the simulation from $t = t_i$ for $t_r = (10^2 \sim 10^3)T_p$. The surface elevation and velocity potential at $t_f = t_i + t_r$ are then recorded as η_f and ϕ_f . Because of the reversibility of the governing equations of oceanic waves, the exact rogue wave will be recovered at $t = t_r$ if we start with the new initial conditions $\eta_0 = \eta_f$ and $\phi_0 = -\phi_f$.

To quantify the error caused by using a homogeneous fluid model in (actually) stratified ocean, we use the exact same new initial conditions η_0 and ϕ_0 as the surface initial conditions to solve wave evolution equations in two layer fluid model, thus $\eta_{u0} = \eta_0$. The dispersion relation for two layer fluid model is

$$\begin{aligned} \mathcal{D}(k, \omega) &= \omega^4 (\mathcal{R} + \coth kh_u \coth kh_\ell) - \\ &\omega^2 gk (\coth kh_u + \coth kh_\ell) + g^2 k^2 (1 - \mathcal{R}) = 0. \end{aligned} \quad (4)$$

For each wave number k , there are two positive ω solutions. The larger one denotes the surface mode and the smaller one denotes the interfacial modes. Each surface mode is a freely propagating wave with a surface elevation and interfacial elevation, so is each interfacial mode. In our considerations, we are assuming that initially all the waves observed on the surface are from surface modes. So initially the interfacial elevation is the elevation due to surface modes only. To initialize the interfacial elevation η_ℓ and interfacial velocity potential ($\phi_u(z = -h_u + \eta_\ell)$ and $\phi_\ell(z = -h_u + \eta_\ell)$) of surface waves, we first break η_{u0} into N waves with amplitude a_n and phase θ_n , and find interfacial amplitude b_n from the linear solution for each of the waves. Then a linear composition of the N waves on the interface is used as initial interfacial wave elevation $\eta_{\ell 0}$. The same method applies in finding interfacial potentials.

Then the wave field is initialized in the two layer fluid model using the new set of initial conditions. The predicted wave field is compared with the original one in the homogeneous fluid model at $t = t_r$. If the predicted rogue wave occurs close enough to the original rogue wave in terms of height, location and time of occurrence, we say the rogue wave is predictable for the specified density ratio \mathcal{R} . Predictability does not require rogue wave to occur at the same time step. In practice, we search for the highest wave in the time span of $t_r - T_p < t < t_r + T_p$ and peak location of rogue wave within $\pm \lambda_p$ from the original rogue wave.

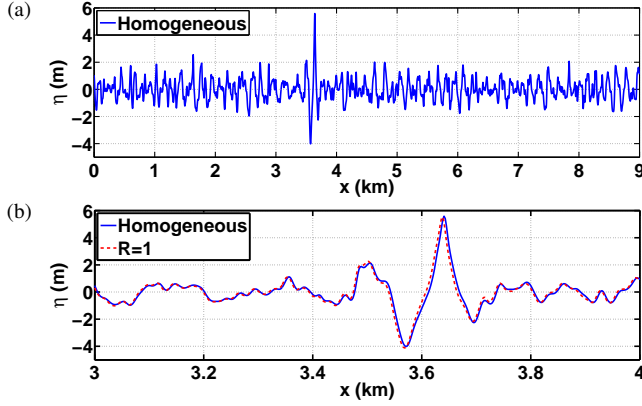


FIGURE 1: (a) One case of the rogue wave predicted in homogeneous fluid. Parameters used in simulation are $M=4$, $N=4096$, $dt = T_p/128$, $H = 300$ m, $T_r = 100T_p$. H_{rs} ratio for this rogue wave is 2.955. (b) Predicted rogue wave in homogeneous fluid (blue line) and two layer fluid (red dash line) with $\mathcal{R} = 1$. $H_{rs}^{(2)} = 2.976$ compared with $H_{rs} = 2.955$. Error=0.7% in terms of predicted H_{rs} ratio. Common simulation parameters are the same as in homogeneous fluid, and $h_u/h = 0.15$. The simulation parameters apply for all the results presented in this paper unless otherwise specified.

We define the maximum wave height to significant wave height ratio of the predicted rogue wave in the two layer fluid model as $H_{rs}^{(2)}$. Then the error is calculated as $Error = (H_{rs}^{(2)} - H_{rs})/H_{rs}$. Rogue wave is predictable if $Error \leq 10\%$. This definition is based on the fact that 10% higher H_{rs} corresponds to waves with an order of magnitude longer return period [28].

First, the rogue wave prediction in the two layer fluid model for $\mathcal{R} = 1$ are compared with the predicted rogue waves in the homogeneous fluid. $\mathcal{R} = 1$ means there is no density variation between the upper layer and lower layer. The velocity field in a homogeneous model is continuous over the whole domain, however, the velocity field near the interface can be discontinuous at the interface of a two-layer density stratified fluid even if $\mathcal{R}=1$. Thus the predicted wave field will not be exactly the same as the homogeneous one. Results for one of the initial conditions from our data base is shown in Fig.1, which represent the general behavior of other initial conditions. We can see that the error for H_{rs} ratio is small enough ($Error < 1\%$). The error is largest at the location of rogue wave, otherwise the error is even smaller. In addition, the predicted rogue wave occurs at almost the same location and time as the original ones.

The predicted rogue wave for density ratios $\mathcal{R} = 0.9, 0.95, 0.97$ and 0.99 are compared with the original ones to investigate the sensitivity of rogue wave prediction to the stratification density ratio, as shown in Fig.2. In the real ocean, $\mathcal{R} = 0.95$ is considered as strongly stratified ocean, larger \mathcal{R} are also consid-

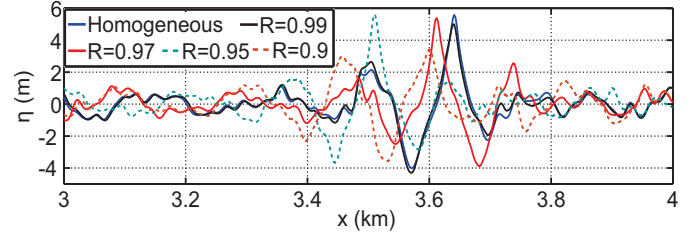


FIGURE 2: Predicted rogue waves for $\mathcal{R} = 0.99, 0.97, 0.95$, and 0.9 . Each line represents the predicted rogue waves in $t_r - T_p < t < t_r + T_p$ and $x_p - \lambda_p < x < x_p + \lambda_p$. $H_{rs}^{(2)}$ is respectively 2.931, 2.883, 2.7864 and 2.19. Error is respectively 0.8%, 2.4%, 5.7% and 25%.

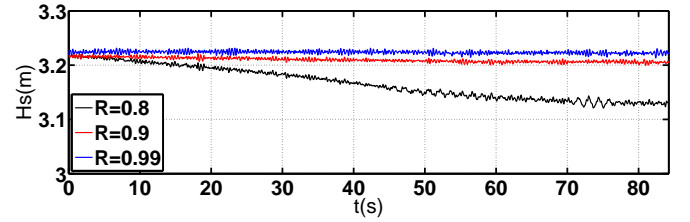


FIGURE 3: Variation of H_s over $100T_p$ for $\mathcal{R} = 0.99, 0.9$ and 0.8 for one particular case. Parameters for sea state 5 is used.

ered to highlight trends. The same surface initial conditions are considered here as those in Fig.1. For $\mathcal{R} = 0.99$, the rogue wave occurs at roughly same location and time with a small error compared with the one in the homogeneous fluid. For $\mathcal{R} = 0.97$, the predicted rogue wave occurs about $0.2\lambda_p$ away from the original rogue wave, where λ_p is the wave length of waves at the peak of spectrum. The $H_{rs}^{(2)}$ ratio is still close to H_{rs} with small error ($\leq 3\%$). For $\mathcal{R} = 0.95$, the predicted rogue wave is about $0.9\lambda_p$ away from the original ones with an error of 5.7%. For $\mathcal{R} = 0.9$, the characteristics of the original rogue wave (wave height and location of occurrence) are distorted. Error is 25% for H_{rs} ratio, which means that rogue wave is not predictable in $100T_p$ for $\mathcal{R} = 0.9$ for this particular initial condition.

It is noted from Fig.3 that H_s is also slowly varying with time. For $\mathcal{R} \leq 0.95$, H_s stays roughly the same. For $\mathcal{R} = 0.9$, the change in H_s is still small. For $\mathcal{R} = 0.8$, the decrease in H_s reaches 1% after $100T_p$.

To obtain the statistical average effect of stratification, a large number of initial conditions ($O(10^2)$) resulting in a rogue wave in $T = 100T_p$ with $H_{rs} = 2 \sim 3$ are considered. Errors for 19 initial conditions are plotted in Fig.4. For density ratios $\mathcal{R} = 0.99, 0.97$ and 0.95 , errors for all the cases are within 10% and it is more deviated from the zero error line for lower density ratios. In addition, error stays roughly the same with different H_{rs} ratios for $\mathcal{R} \geq 0.95$. For $\mathcal{R} = 0.9$, error becomes larger

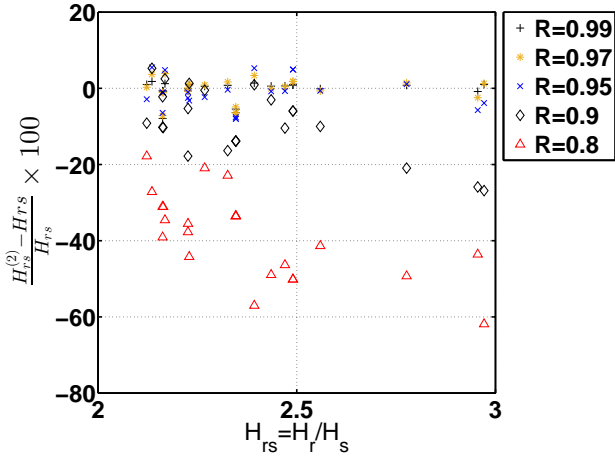


FIGURE 4: Error with respect to H_{rs} ratio in $100 T_p$ for $\mathcal{R} = 0.99, 0.97, 0.95, 0.9$ and 0.8 . Markers with the same H_{rs} ratio have the same surface initial condition (wave elevation and surface potential). Each marker with the same color represents the error for one specific initial condition.

than 10%, and we can see that error is larger on average for a larger H_{rs} ratio, which can reach up to more than 20%. Error for $\mathcal{R} = 0.8$ can reach up to more than 60% and it also increases as H_{rs} ratio increases. Although $\mathcal{R} = 0.8$ is not likely to represent the real stratified ocean, it is still considered here to evaluate the general effect of stratification. It may have applications in other contexts. For sea state 5, rogue wave is predictable in $100T_p$ for density ratio $\mathcal{R} \geq 0.95$. It is to be noted that even if the simulation using the homogeneous fluid model based on current sea state model predicts no rogue wave occurrence in $100T_p$, rogue wave may occur in strongly stratified fluid since the wave characteristics are changed.

The predictability also relies on how far ahead we need to predict. All the research work above is based on prediction in $100T_p$. To be more specific, after we found the rogue wave, we continue the simulation for $100T_p$ and $500T_p$ respectively. Then the new initial conditions are used in the homogeneous fluid model and the two layer fluid model for simulation for $100T_p$ and $500T_p$ respectively to evaluate the error in the recovered rogue wave. If we want to predict rogue wave in longer time, the predictability on the limit of stratification ratio is different. In this paper, we consider many initial conditions resulting in rogue wave in $100T_p$ and $500T_p$ in the homogeneous fluid. For the two layer fluid model, $\mathcal{R} = 0.99, 0.9$ and 0.8 ratios are used. From the results in Fig.5, we can see that error in $500T_p$ can reach up to 60% compared with 25% in $100T_p$ for $\mathcal{R}=0.9$. For $\mathcal{R}=0.99$, the error in $500T_p$ can reach up to 20%. However, this error in $100T_p$ is less than 10%. Errors for $\mathcal{R}=0.8$ in $100T_p$ and $500T_p$ are both very large. If rogue wave in longer time needs to be pre-

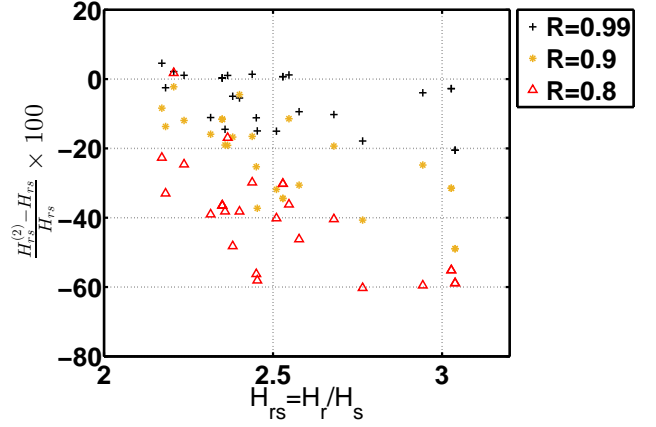


FIGURE 5: Error with respect to H_{rs} ratio in $500T_p$ for $\mathcal{R} = 0.99, 0.95$ and 0.9 .

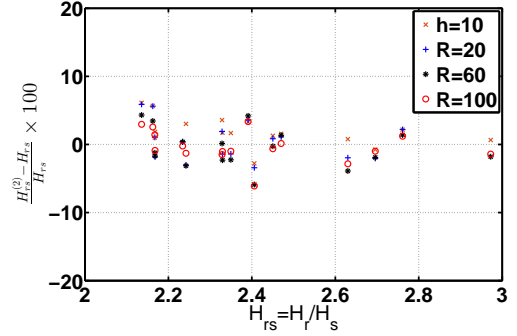


FIGURE 6: Error for $\mathcal{R}=0.95$ in $100T_p$ for three upper layer depth, $h_u = 10, 20, 60, 100$ m. The total water depth is 300 m.

dicted, the error is larger. The wave field is, thus, more deviated from the original one.

The sensitivity of ocean rogue wave prediction also depends on the depth ratio (h_u/h) in stratified fluid. Four h_u values 10, 20, 60 and 100 m are considered for a fixed density ratio 0.95 and fixed depth $h = 300$ m, as shown in Fig.6. For this given density ratio, the predicted rogue wave is not very sensitive to upper layer depth change. The maximum error is less than 10%, which satisfies the requirements on predictable rogue wave. For $h_u = 10$ m, the error ratio is scattering further away from zero error line, which means that the predicted rogue wave is more deviated from the original ones. For $h_u = 60$ m and $h_u = 100$ m, the predicted rogue wave has smaller average error.

CONCLUSIONS

We investigated the predictability of the oceanic rogue wave in stratified fluid based on statistical analysis and calculate the

error caused by stratification. The energy transfer occurs in stratified ocean between surface gravity waves and internal waves may explain why the predicted rogue wave is different from the one in homogeneous fluid. In the two layer stratified fluid, one surface wave can interact with another surface wave to generate a new interfacial wave mode. Then the new interfacial wave mode can again interact with other surface waves to generate more wave modes. In this way, the energy can be transferred between surface wave and interfacial wave. A two layer stratified ocean model is used with different density ratios. It is shown that for $\mathcal{R} \geq 0.95$, rogue wave is predictable (with an error less than 10%) in $100T_p$. As the stratification becomes even stronger ($\mathcal{R} = 0.9$ and 0.8), the error becomes large and increases as the H_{rs} ratio increases. For the given two layer stratified ocean, the error will be larger if rogue wave needs to be predicted further in the future. Predicted rogue wave in $500T_p$ and $100T_p$ ahead of time are compared for $\mathcal{R} = 0.9$. For $\mathcal{R} = 0.95$, prediction of ocean rogue wave is not very sensitive to varying upper layer depth. The present study gives insight to oceanic rogue wave prediction because it takes into account the fact that the ocean is stratified.

REFERENCES

- [1] Draper, L., 1967. ““Freak” ocean waves”. *Oceanus*, **10**, pp. 13–15.
- [2] Draper, L., 1971. “Severe wave conditions at sea”. *Journal of the Institute of Navigation*, **24**(3), pp. 273–277.
- [3] Kharif, C., and Pelinovsky, E., 2003. “Physical mechanisms of the rogue wave phenomenon”. *European Journal of Mechanics - B/Fluids*, **22**(6), Nov., pp. 603–634.
- [4] Liu, P., 2007. “A chronology of freak wave encounters”. *Geofizika*, **24**(1).
- [5] Didenkulova, I., 2006. “Freak waves in 2005”. *Natural Hazards Earth Syst. Sci.*(1998), pp. 1007–1015.
- [6] Muir, L. R., and a.H. El-Shaarawi, 1986. “On the calculation of extreme wave heights: A review”. *Ocean Engineering*, **13**(1), Jan., pp. 93–118.
- [7] Akhmediev, N., Ankiewicz, a., and Taki, M., 2009. “Waves that appear from nowhere and disappear without a trace”. *Physics Letters A*, **373**(6), Feb., pp. 675–678.
- [8] Guedes Soares, C., Cherneva, Z., and Antao, E. M., 2003. “Characteristics of abnormal waves in North Sea storm sea states”. *Applied Ocean Research*, **25**(2003), pp. 337–344.
- [9] Lavrenov, I. V., 1998. “The wave energy concentration at the Agulhas Current off South Africa”. *Natural Hazards*, **17**, pp. 117–127.
- [10] Garrett, C., and Munk, W., 1979. “Internal Waves in the Ocean”. *Annual Reviews in Fluid Mechanics*, **11**(1), Jan., pp. 339–369.
- [11] Sigman, D. M., Jaccard, S. L., and Haug, G. H., 2004. “Polar ocean stratification in a cold climate”. *Nature*, **428**(6978), pp. 59–63.
- [12] Holt, J. T., and Thorpe, S. A., 1997. “The propagation of high frequency internal waves in the Celtic Sea”. *Deep-Sea Research Part I*, **44**(12), pp. 2087–2116.
- [13] Choi, W., and Camassa, R., 1996. “Long Internal Waves of Finite Amplitude”. *Physical review letters*, **77**(9), Aug., pp. 1759–1762.
- [14] Boegman, L., Imberger, J., Ivey, G. N., Antenucci, J. P., and Hogg, A., 2003. “High-frequency internal waves in large stratified lakes acknowledge data processing”. *Limnology*, **48**(2), pp. 895–919.
- [15] Dommermuth, D. G., and Yue, D. K. P., 1987. “A high-order spectral method for the study of nonlinear gravity waves”. *Journal of Fluid Mechanics*, **184**, Apr., p. 267.
- [16] LIU, Y., and YUE, D. K., 1998. “On generalized Bragg scattering of surface waves by bottom ripples”. *Journal of Fluid Mechanics*, **356**, pp. 297–326.
- [17] Hasselmann, K., Barnett, T., Bouws, E., and Carlson, H., 1973. “Measurements of wind-wave growth and swell decay during the Joint North Sea Wave Project”. *Deutsches Hydrographisches Institut - Hamburg*.
- [18] Carter, D., 1982. “Prediction of wave height and period for a constant wind velocity using the JONSWAP results”. *Ocean engineering*, **9**(1), pp. 17–33.
- [19] Alam, M.-R., Liu, Y., and Yue, D. K. P., 2009. “Bragg resonance of waves in a two-layer fluid propagating over bottom ripples. Part II. Numerical simulation”. *Journal of Fluid Mechanics*, **624**, Mar., p. 225.
- [20] Alam, M.-R., Liu, Y., and Yue, D. K. P., 2009. “Waves due to an oscillating and translating disturbance in a two-layer density-stratified fluid”. *Journal of Engineering Mathematics*, **675**(2), June, pp. 179–200.
- [21] Alam, M.-R., Liu, Y., and Yue, D. K. P., 2010. “Oblique sub- and super-harmonic Bragg resonance of surface waves by bottom ripples”. *Journal of Fluid Mechanics*, **643**, Jan., pp. 437–447.
- [22] Toffoli, a., Gramstad, O., Trulsen, K., Monbaliu, J., Bitner-Gregersen, E., and Onorato, M., 2010. “Evolution of weakly nonlinear random directional waves: laboratory experiments and numerical simulations”. *Journal of Fluid Mechanics*, **664**, Oct., pp. 313–336.
- [23] Alam, M.-R., 2012. “A new triad resonance between co-propagating surface and interfacial waves”. *Journal of Fluid Mechanics*, **691**, Dec., pp. 267–278.
- [24] Alam, M.-R., 2012. “Broadband Cloaking in Stratified Seas”. *Physical Review Letters*, **108**(8), Feb., pp. 1–4.
- [25] Alam, M.-R., 2012. “Nonlinear analysis of an actuated seafloor-mounted carpet for a high-performance wave energy extraction”. *Proceedings of the Royal Society A: Mathematical, Physical and Engineering Sciences*. doi 10.1098/rspa.2012.0193, June.

- [26] Alam, M.-r., 2014. “Predictability horizon of oceanic rogue waves”. *Geophysical Research Letters*, **41**, pp. 1–9.
- [27] Wu, G., 2004. “Direct simulation and deterministic prediction of large-scale nonlinear ocean wave-field”. PhD thesis, Massachusetts Institute of Technology, Cambridge, MA.
- [28] Leonard-Williams, A., and Saulter, A., 2013. Comparing EVA results from analysis of 12 years of WAVEWATCHIII and 50 years of NORA10 data. Tech. Rep. February.